LRP 362/88 November 1988

IDEAL STABILITY OF CYLINDRICAL PLASMA IN THE PRESENCE OF MASS FLOW

A. Bondeson and R. Iacono

Paper submitted to Physics of Fluids

IDEAL STABILITY OF CYLINDRICAL PLASMA IN THE PRESENCE OF MASS FLOW

A. Bondeson and R. Iacono

Centre de Recherches en Physique des Plasmas
Association Euratom - Confédération Suisse
Ecole Polytechnique Fédérale de Lausanne
21 Av. des Bains, CH-1007 Lausanne
Switzerland

Abstract: The ideal stability of cylindrical plasma with mass flows is investigated using the guiding centre plasma (GCP) model of Grad. For rotating plasmas, the kinetic treatment of the parallel motion in GCP gives significantly different results than fluid models, where the pressures are obtained from equations of state. In particular, GCP removes the resonance with slow magnetoacoustic waves and the loss of stability that results in magnetohydrodynamics (MHD) for near-sonic flows. Because of the strong kinetic damping of the sound waves in an isothermal plasma, the slow waves have little influence on plasma stability in GCP at low β. In the large aspect ratio, low-β tokamak ordering, Alfvénic flows are needed to change the ideal GCP stability significantly. At lowest order in the inverse aspect ratio, flow can be favorable or unfavorable for stability of local modes depending on the profiles, but external kinks are always destabilized by flow if the velocity vanishes at the edge. For high-β, reversed field pinch equilibria, numerical computations show that flow can be stabilizing for local modes, but external modes are destabilized by flow. It is shown that in three dimensions, the MHD equilibrium problem becomes hyperbolic for arbitrarily small flows across the magnetic field, whereas in GCP the equilibrium equation remains elliptic for sub-Alfvénic flows.

I. Introduction

In contrast with static plasma equilibria, where a detailed picture has been established for the the macroscopic stability of various devices, little is known at present about the stability of equilibria with mass flows. Nevertheless, the stability of rotating plasmas has become a question of practical importance in fusion research because of the substantial neutral beam power in recent tokamak experiments,[1-3] available not only to heat the plasma, but also to produce mass flows. Naturally, plasma flows frequently play important roles in astrophysical and geophysical contexts.[4,5]

In this paper, we investigate the ideal linear stability of cylindrical equilibria with arbitrary profiles of magnetic fields and mass flow. Previous studies[6-8] based on magnetohydrodynamics (MHD) predicted that flows of the order of the sound speed lead to complete loss of stability because of resonance with slow magneto-acoustic waves. However, there is experimental evidence that the sound speed does not present a stability limit, e.g., from the F-II device in Stockholm.[9] In addition, it is well known[10] that the MHD equations poorly describe the slow magneto-acoustic and ion-sound waves by assuming an equation of state, $p \propto \rho^{\gamma}$. A semi-macroscopic theory better suited for the description of rotating plasmas is the guiding centre plasma (GCP) model of Grad.[11] The GCP model is identical to MHD for plasma motion across the magnetic field, but uses kinetic theory to describe the motion of particles along the field lines. It introduces Landau damping of the sound waves, which strongly reduces their effect on plasma stability, and indeed removes the MHD stability limit at the sound speed.

In Sec. II, we derive the second order radial eigenvalue problem, including the effects of mass flow for several different models: GCP, MHD (including parallel viscosity) and the double adiabatic theory of Chew, Goldberger and Low[12] (CGL). The difference between these descriptions lies in three coefficients, expressing the response in plasma density and perpendicular pressure to perturbations of the parallel magnetic field and to radial displacements. In the inviscid fluid models, the plasma response shows a resonance when the parallel phase speed of the mode in the local centre of mass frame equals the sound speed. This resonance is removed in GCP by the kinetic

treatment of the parallel motion, and the influence of the magneto-acoustic wave on the stability of rotating plasmas is much reduced. As a consequence, the sound speed does not set a stability limit in GCP. The resonance is also removed by adding parallel viscosity in the MHD equations, as was done in a recent calculation by Gimblett.[13] However, for frequencies larger than the ion-ion collision frequency, the response of the viscous MHD plasma is quite different from that of GCP. An interesting result is that at marginal stability and in the absence of flow, the response of the guiding centre model for a plasma in local thermodynamic equilibrium is identical to that of inviscid MHD with the adiabatic index γ set to unity, and differs from the double-adiabatic approximation. Thus, for static equilibria, MHD and GCP predict the same marginal points, whereas CGL is more optimistic.

In Sec. III, we consider the stability of local modes and find that whenever the flow has shear, the GCP description leads to a complex Suydam parameter. This implies that the infinite sequences of unstable modes occurring in MHD when the Suydam criterion is violated do not exist in GCP with sheared flows (although they do occur for static equilibria, as shown by Pao[14]). For an equilibrium of reversed field pinch (RFP) type, we find numerically that flow is stabilizing for the local modes, apparently due to the kinetic damping in GCP. However, in the limit of low-β, large aspect ratio tokamaks, the flow must be Alfvénic to give an O(1) contribution to the Suydam index. This contribution can be stabilizing if the pitch of the flow is opposite to that of the magnetic field.

In Sec. IV, we consider global modes, in particular external kinks, and use the "straight tokamak" or lowest order reduced-MHD ordering to study the effects of Alfvénic flows. In lowest order, the slow waves are eliminated completely in GCP. An integral expression, analogous to δW, is derived for modes locked to resistive walls. This expression shows that any flow that vanishes at the plasma surface is destabilizing for wall-locked external kinks. Numerical computations confirm this conclusion also for RFP equilibria and for internal kink modes.

In Sec. V, we discuss properties of equilibria with flow by applying the linearized eigenvalue problem to perturbations with zero frequency in the laboratory frame. As is

well known,[15] the MHD Grad-Shafranov equation can become hyperbolic because of mass flow, and there exists a "first hyperbolic region" where the poloidal flow is close to the poloidal sound-speed. We show that in three dimensions, the introduction of arbitrarily small flows perpendicular to the magnetic field makes the MHD equilibrium equation hyperbolic. However, the guiding centre plasma has very different properties, and the equilibrium equation remains elliptic for sub-Alfvénic flows. This difference was noted for axisymmetric equilibria in a guiding centre calculation by Dobrott and Greene.[16] The absence of the "first hyperbolic region" in the GCP equilibrium problem as well as the absence of pronounced degradation of stability for sonic flows are both due to the near-elimination of the slow magneto-acoustic wave in a kinetic description.

II. The radial eigenvalue problem

It is well known[10] that MHD does not properly describe slow magneto-acoustic waves in collisionless, isothermal plasma, and that the equation of state, $p \propto \rho^{\gamma}$, can only be justified in the limit of large collisionality, $\nu_{ii} >> |\tilde{\omega}|$, where $\tilde{\omega}$ stands for the wave frequency in the local center of mass frame. The double adiabatic theory of Chew, Goldberger and Low[12] lacks another important piece of physics by ignoring the heat flow along the field lines, and only holds in the limit of large phase velocity, $|\tilde{\omega}| >> \max(k_{||} v_{the}, \nu_{ii})$. Similar to MHD, it fails to produce damping of the ion-sound waves. As ion-sound waves play a prominent role for the MHD stability of rotating plasmas,[7] a more adequate model for the flow problem is the guiding centre plasma (GCP) model of Grad.[11] GCP uses kinetic theory for the motion along the field lines and assumes no ordering of the parallel phase velocity with respect to the thermal velocities. The slow magnetosonic wave has very different properties in MHD and GCP,[10] and in the kinetic description, the magnetosonic wave is almost eliminated in isothermal plasma. Here, we show that this modification of the slow wave physics has significant consequences for the stability of plasmas with sheared flows, viz., the MHD instability induced by resonance with slow waves[7] is removed and, with it, the unconditional instability for near-sonic flows.

We now derive the second order cylindrical eigenvalue problem[17] for GCP, previously stated in Ref 18. We first treat the fluid part of the calculation, leaving the pressures unspecified. This allows us to substitute either the MHD, CGL or GCP model for the parallel motion and compare the results simply by substituting different forms for three coefficients into the second order radial equation. The same approach is taken in a companion paper on toroidal equilibrium.[19] The reader not interested in details may omit the derivation in Secs. II.A-B.

II.A Fluid calculation

The linearized MHD equations for equilibria with mass flow were given by Frieman and Rotenberg.[20] We generalize their model by allowing for anisotropic pressure

$$\rho \frac{\partial^2 \underline{\xi}}{\partial t^2} + 2\rho\, \underline{v}\cdot\nabla \frac{\partial \underline{\xi}}{\partial t} = -\nabla\cdot (\underline{\underline{P}} + \underline{\underline{I}}\, \underline{B}\cdot\underline{Q}) + \underline{B}\cdot\nabla\underline{Q} + \underline{Q}\cdot\nabla\underline{B}$$

$$+ \nabla\cdot [\rho\underline{\xi}(\underline{v}\cdot\nabla)\underline{v} - \rho\underline{v}(\underline{v}\cdot\nabla)\underline{\xi}] \quad , \tag{1}$$

$$\underline{\underline{P}} = (p_\perp \underline{\underline{I}} + \frac{p_\parallel - p_\perp}{B^2} \underline{B}\,\underline{B})_1 \quad . \tag{2}$$

Here, $\underline{\xi}$ is the Lagrangean displacement, subscript "1" denotes Eularian perturbed quantities and $\underline{Q} = \underline{B}_1$. In the following we make extensive use of Lagrangean perturbations, such as

$$\delta\underline{v} = \underline{v}_1 + \underline{\xi}\cdot\nabla\underline{v} = (\frac{\partial}{\partial t} + \underline{v}\cdot\nabla)\,\underline{\xi} \quad , \tag{3a}$$

$$\delta\rho = \rho_1 + \underline{\xi}\cdot\nabla\rho = -\rho\,\nabla\cdot\underline{\xi} \quad , \tag{3b}$$

$$\delta\underline{B} = \underline{Q} + \underline{\xi}\cdot\nabla\underline{B} = \underline{B}\cdot\nabla\underline{\xi} - \underline{B}\,\nabla\cdot\underline{\xi} \quad , \tag{3c}$$

The equilibrium relation in a cylinder reads

$$\frac{d}{dr}\left(p_\perp + \frac{B^2}{2}\right) = (\rho v_\theta^2 - \sigma B_\theta^2)/r \quad , \tag{4a}$$

where

$$\sigma = 1 - \Delta = 1 - \frac{p_\parallel - p_\perp}{B^2} \quad . \tag{4b}$$

Assuming an exp[i(ωt+mθ-kz)] dependence for the perturbed variables, we obtain from (1) using (3b,c)

$$A\,\underline{\xi} + \hat{r}\left[r\xi_r \frac{d}{dr}\left(\frac{\sigma B_\theta^2 - \rho v_\theta^2}{r^2}\right) - \frac{\delta\rho}{\rho}\,\frac{\sigma B_\theta^2 - \rho v_\theta^2}{r}\right]$$

$$+ \frac{2iT}{r}\,\hat{z}\times\underline{\xi} = \nabla p_* - \left(iF\underline{B} - \hat{r}\,B_\theta^2/r\right)(\delta\sigma + \sigma\,\delta\rho/\rho) \quad , \tag{5}$$

where

$$p_* = p_{\perp 1} + \underline{B}\cdot\underline{Q} \tag{6}$$

is the perturbation in total perpendicular pressure. The coefficients in Eq.(5) are given by

$$\begin{aligned} A &= \rho\tilde{\omega}^2 - \sigma F^2 \quad , \\ T &= \sigma F B_\theta - \rho\tilde{\omega} v_\theta \quad , \\ F &= \underline{k}\cdot\underline{B} = k_\parallel B = mB_\theta/r - kB_z \quad , \\ \tilde{\omega} &= \omega + \underline{k}\cdot\underline{v} = \omega + mv_\theta/r - kv_z \quad , \end{aligned} \tag{7}$$

and $\tilde{\omega}$ is the Doppler shifted frequency. In Eq. (5), all information about the parallel dynamics is contained in $\delta\rho$, p_* and $\delta\sigma$. The perturbed magnetic field has been eliminated except for the parallel component δB, appearing in $\delta\sigma$. [Derivatives of equilibrium quantities could be entirely eliminated from (5) by using $\delta(p_\perp + B^2/2)$ instead of p_*, but this would make the final eigenvalue equation appear somewhat more complicated.]

The displacement is decomposed according to

$$\underline{\xi} = \xi_r \hat{r} + \xi_\perp \frac{\hat{r} \times \underline{B}}{B} + \xi_{||} \frac{\underline{B}}{B} \quad . \tag{8}$$

Simple consequences of (3b,c) are

$$B\,\delta B = iEB\xi_\perp - \frac{B^2}{r}\frac{d}{dr}(r\xi_r) + \frac{B_\theta^2}{r}\xi_r \quad , \tag{9a}$$

$$\frac{\delta B}{B} - \frac{\delta\rho}{\rho} = ik_{||}\xi_{||} + \frac{B_\theta^2}{rB^2}\xi_r \quad , \tag{9b}$$

where

$$E = mB_z/r + kB_\theta = \hat{r} \cdot (\underline{k} \times \underline{B}) = k_\perp B \quad . \tag{10}$$

The equation of motion, written componentwise, reads

$$\left[A + r\frac{d}{dr}\left(\frac{\sigma B_\theta^2 - \rho v_\theta^2}{r^2}\right) + \frac{B_\theta^2}{r^2B^2}\frac{2TB_\theta}{F}\right]\xi_r + \frac{\delta\rho}{r}\left(X^2 - \frac{\tilde{\omega}^2 B_\theta^2}{F^2}\right)$$

$$+ \frac{2iTB_z}{rB}\xi_\perp = \frac{dp_*}{dr} + \frac{2TB_\theta}{rF}\frac{\delta B}{B} + \frac{B_\theta^2}{rB^2}\left[\delta p_\perp - \delta p_{||} + 2\Delta B\,\delta B\right] \quad , \tag{11}$$

$$AB\,\xi_{\perp} = \frac{2iTB_z}{r}\,\xi_r - iEp_* \quad , \qquad (12)$$

$$\rho\tilde{\omega}^2\left(iFB\,\xi_{||} + \frac{B_\theta^2}{r}\xi_r \right) = F^2\left(\Delta B\,\delta B - \delta p_{||} + \frac{\rho X^2}{r}\,\xi_r \right) \quad , \qquad (13)$$

where

$$X = v_\theta - \tilde{\omega}B_\theta/F \qquad (14)$$

is related to the crossfield flow of the equilibrium. Substituting (9b) in the parallel momentum equation (13), we can eliminate $\xi_{||}$ and obtain a relation between the perturbations in parallel pressure, density and magnetic field

$$k_{||}^2\left(\delta p_{||} - \Delta B\,\delta B - \frac{\rho X^2}{r}\xi_r \right) = \rho\tilde{\omega}^2\left(\frac{\delta\rho}{\rho} - \frac{\delta B}{B} \right) \quad . \qquad (15)$$

II.B Parallel dynamics

To close the system (11-13), we must express $\delta\rho$ and $\delta p_{\perp}$ in terms of δB and ξ_r. In the MHD and double adiabatic equations this is accomplished by substituting the respective equations of state in the parallel equation of motion (15), as shown in Appendix B. In Grad's guiding centre model,[11] the motion along the field lines is treated kinetically. All particles are assumed to have the same velocity $\underline{U} = \underline{E} \times \underline{B}/B^2$ perpendicular to the magnetic field, but each particle has its own velocity V along $\hat{b} = \underline{B}/B$, satisfying

$$\frac{dV}{dt} = \frac{e}{m}E_{||} + \hat{b}\cdot\nabla\left(\frac{U^2}{2} - \mu B\right) + V\,\underline{U}\cdot(\hat{b}\cdot\nabla\hat{b}) \quad . \qquad (16)$$

Here, e and m denote the charge and mass of the particle, and μ is its magnetic moment, $v_\perp^2/B$. e/m is regarded as a large parameter, and $E_{||}$ is neglected in Faraday's law. The parallel electric field is determined selfconsistently by demanding that the electrical current computed from (16) vanish, $j_{||} = \Sigma\, (e_\ell/m_\ell)\, \rho_\ell \langle V_\ell \rangle = 0$, where ℓ denotes the different species. Because of the large parameter e/m, this does not imply that $\underline{B} \cdot \nabla \times \underline{B}$ is zero, only that it is $O((e/m)^0)$.

The kinetic equation for the linearized Eq. (16) can be written, after considerable algebra,

$$\left(\delta f - \frac{\delta B}{B} f_0 + \frac{\kappa}{k_{||}} \frac{\partial f_0}{\partial V} \right)$$

$$- \left[\frac{e}{m} E_{||} + i k_{||} \left(\frac{X^2}{r} \xi_r - \mu\, \delta B \right) \right] \frac{i\, \partial f_0 / \partial V}{\tilde{\omega} + k_{||} V_s} = 0 \quad , \tag{17}$$

where $V_s = V - V_0$, $V_0 = \underline{v} \cdot \hat{b}_0$ is the equilibrium mass velocity along the field lines and $\kappa = [\underline{U} \cdot (\underline{B} \cdot \nabla \underline{B})]_1 / B^2$. The parallel motion is driven primarily by the force on a magnetic dipole and a fluid force that originates from equilibrium flow perpendicular to the magnetic field. The curvature term drops out when $\delta\rho$ and $\delta p_\perp$ are calculated:

$$(\delta\rho\, ,\, \delta p_\perp - p_\perp\, \delta B/B) = \sum_{\ell} \int \delta f_\ell (1, \mu B)\, d\mu\, dV \quad .$$

$E_{||}$ is eliminated by means of the parallel current constraint, $j_{||} = O((e/m)^0)$, evaluated by multiplying (17) by e_ℓ/m_ℓ and integrating,

$$E_{||} \sum_{\ell} (e_\ell/m_\ell)^2\, J_{\ell,0} = i k_{||} \sum_{\ell} (e_\ell/m_\ell) \left[\delta B\, J_{\ell,1} - \frac{X^2}{r} \xi_r\, J_{\ell,0} \right] . \tag{18}$$

Here

$$J_{\ell,n} = \int \frac{\mu^n}{V_s - V_p} \frac{\partial f_{0\ell}}{\partial V}\, d\mu\, dV \quad , \tag{19}$$

and

$$V_p = -\tilde{\omega}/k_{||} \tag{20}$$

is the parallel phase velocity in the frame moving with the plasma. After elimination of $E_{||}$, we have

$$\begin{aligned} \delta p_\perp - \frac{2\delta B}{B} p_\perp &= a_1 B\delta B - a_2 \frac{\rho X^2}{r} \xi_r \quad , \\ \delta\rho - \frac{\delta B}{B}\rho &= a_3 \rho \frac{\delta B}{B} - a_4 \frac{\rho X^2}{r} \xi_r \quad , \end{aligned} \tag{21}$$

where the coefficients are given by

$$\begin{aligned} a_1 &= I_{2,0} - I_{1,1} I_{1,1} / I_{0,2} \quad , \\ a_2 = a_3 &= B\rho^{-1} (I_{1,0} - I_{1,1} I_{0,1} / I_{0,2}) \quad , \\ a_4 &= \rho^{-1} (I_{0,0} - I_{0,1} I_{0,1} / I_{0,2}) \quad , \end{aligned} \tag{22}$$

and

$$I_{n,m} = \sum_{\ell} (e_\ell/m_\ell)^m J_{\ell,n} \quad . \tag{23}$$

In Appendix A we discuss the question of energy conservation in the linearized GCP system and show that this system has an energy integral when the kinetic damping vanishes. In Appendix B, we derive the coefficients a_1 through a_4 for fluid models with an equation of state. For these models, the condition for energy conservation can be formulated as a condition on the partial derivatives of $p_{||}$ and $p_\perp$ with respect to ρ and B. This condition is, of course, satisfied by both MHD and double adiabatic approximation.

II.C Plasma response in GCP, MHD and CGL

For a plasma in local thermodynamic equilibrium ($p_{||} = p_{\perp} = p$, $p_e = p_i = p/2$, and Maxwellian distributions), the coefficients (22) become

$$a_1 = -\frac{p}{B^2}\left[\chi_e + \chi_i - \frac{(\chi_e - \chi_i)^2}{2(\chi_e + \chi_i)}\right] \quad , \qquad (24a)$$

$$a_2 = -\frac{2\chi_e\chi_i}{\chi_e + \chi_i} \quad , \qquad a_4 = \frac{\rho}{p}\, a_2 \quad ,$$

where

$$\chi = 1 + \zeta\, Z(\zeta) \quad , \qquad \zeta = -\frac{\tilde{\omega}}{|k_{||}|\sqrt{2}v_{th}} \quad , \qquad (24b)$$

and Z is the Fried-Conte plasma dispersion function.[21] This form for the coefficients is assumed for the numerical examples throughout this paper and leads to strong kinetic damping of the ion sound and slow magneto-acoustic waves. Sound-waves of a hydrodynamic character can, of course, be recovered if $T_e >> T_i$.

It is of interest to compare the plasma responses of the various models GCP (24), MHD [$p_{||} = p_{\perp} = p$ and $\delta(p/\rho^{\gamma}) = 0$], CGL [$\delta(p_{\perp}/\rho B) = 0$ and $\delta(p_{||}B^2/\rho^3) = 0$] and MHD with a large parallel viscosity. In the case of small phase velocity, $|V_p| << |v_{thi}|$, the coefficients are as given in Table 1. Here, it has been assumed that the electron and ion temperatures are equal, but not isotropic, and the distributions have been taken as bimaxwellians. For the viscous MHD coefficients, the parallel viscosity has been assumed infinite, i.e., we consider the response on time-scales much shorter than the collision time. We note that whereas the CGL equations reproduces the same type of dependence on $p_{\perp}/p_{||}$ as the guiding centre model, the numerical coefficients are incorrect. This is not surprising since the CGL equations ignore the heat flux along the

field lines and only apply in the limit of large phase velocity. It is perhaps more surprising and of more significance that MHD with the adiabatic index γ set to unity, exactly reproduces GCP for isotropic equilibria. It follows that for static equilibria (with finite shear) MHD, but not CGL, gives the same marginal point as GCP. The reason for the difference is that the CGL equations do not allow the temperatures to equilibrate along the field lines, contrary to the case of zero phase velocity in GCP and MHD with γ=1. [For static equilibria, only the value of a_1 is significant at marginal stability, and a_2, a_4, and hence γ, are immaterial. However, for special types of flow, such as rigid rotation, where marginal stability also occurs at V_p=0, the coefficients related to compressibility do influence the marginal point, see Appendix C.]

In general when the equilibrium has mass flows, the parallel phase velocity is nonzero. In the inviscid fluid models, the coefficients a_1 through a_4 have singularities when the phase velocity equals the sound speed. These singularities are smeared out in GCP, and the GCP coefficients have large imaginary parts due to wave-particle resonance around the thermal speed, which introduce damping in the macroscopic system. To emphasize the difference between GCP, MHD and CGL, Fig. 1 shows $1+a_2(V_p)$, which gives the density response to a perturbation in the parallel magnetic field. We note (a) the unphysical resonances and the absence of imaginary part in the fluid models, (b) that CGL deviates from GCP already in the static case $V_p = 0$, and (c) that for small but finite phase velocity, the MHD coefficient not only ignores the dominant imaginary part, but also gives the opposite sign as GCP for the real part. It is obvious that fluid models can give spurious results for equilibria with mass flows, in particular, when the phase velocity of a mode is near the ion thermal speed.

II.D The radial eigenvalue problem

Given the expressions (21) for $\delta\rho$ and $\delta p_\perp$ we can now close the system (11-13) and derive a pair of first order equations for ξ_r and p_*.[17] We first substitute the expression (21) for $\delta p_\perp$ into the definition of p_* and obtain

$$p_* = K\, B\delta B + H\, \xi_r/r \quad , \tag{25}$$

where

$$\begin{aligned} K &= 1 + \frac{2p_\perp}{B^2} + a_1 \quad , \\ H &= \sigma B_\theta^2 - \rho v_\theta^2 - a_2\, \rho X^2 \quad . \end{aligned} \tag{26}$$

According to (25), K may be interpreted as the perturbation in total perpendicular pressure $p_\perp + B^2/2$ due to a unit perturbation in magnetic pressure $B^2/2$. An equation for $d\xi_r/dr$ is obtained directly from (25) using (9a) for δB and (12) for $\xi_\perp$, and dp_*/dr is computed from the radial equation of motion (11) [substituting (15) , (21) and (25)]

$$\begin{aligned} \frac{1}{r}\frac{d}{dr}(r\xi_r) &= C_1\, \xi_r - C_2\, p_* \quad , \\ \frac{dp_*}{dr} &= C_3\, \xi_r - C_1\, p_* \quad . \end{aligned} \tag{27}$$

The coefficients in (27) are given by

$$C_1 = \frac{1}{rB^2}\left(-\frac{2TB_z E}{A} + B_\theta^2 + \frac{H}{K}\right) \quad , \tag{28a}$$

$$C_2 = \frac{1}{B^2}\left(-\frac{E^2}{A} + \frac{1}{K}\right) \quad , \tag{28b}$$

$$C_3 = A + r\frac{d}{dr}\left(\frac{\sigma B_\theta^2 - \rho v_\theta^2}{r^2}\right) - \frac{4B_z^2T^2}{r^2B^2A}$$

$$- a_4\frac{\rho X^4}{r^2} + \frac{1}{r^2B^2}\left[\frac{H^2}{K} + \frac{B_\theta^3}{F^2}(B_\theta A + 4FT)\right] \quad . \tag{28c}$$

Equations (26-28) give the MHD,[7] viscous MHD,[13] CGL, and GCP[18] eigenvalue problems by substitution of the appropriate coefficients a_1, a_2 and a_4 from (22), (B2) or (B5). The system is manifestly Hamiltonian in $r\xi_r$ and p_*. This property would be lost if the symmetry $a_2 = a_3$ (22) [for the fluid models, condition (B1)] was violated. The Hamiltonian character of (26-28) has certain mathematical advantages, such as allowing a strong variational form as we exploit in Sec. IV A.

The information concerning the parallel dynamics is contained in K, H and a_4, and we reiterate that in the fluid models, these show unphysical resonances at the sound speed. The resonances do not lead to singularity of the radial equation, because of interrelations between the coefficients (B2). However, true singularities occur at the zeroes of K, corresponding to the slow wave continua. In the inviscid fluid models the zeroes of K occur for real frequencies; e.g.,

$$K^{MHD} = 1 + \frac{\beta V_p^2}{V_p^2 - v_s^2}$$

with $v_s^2 = \gamma p/\rho$ and $\beta = \gamma p/B^2$, has zeroes at $V_p^2 = v_s^2/(1+\beta)$ close to its poles at $V_p^2 = v_s^2$. The important difference between the fluid models and GCP is that with the kinetic description of the parallel motion, the poles of a_1 and the zeroes of K lie in the stable halfplane, if the distribution function is locally stable. Hence, for real ω, K^{GCP} is uniformly $1 + O(\beta)$.

In Sec. V, we discuss the problem of equilibrium in two and three dimensions and show that the question of ellipticity for the equilibrium equation can be answered by

inspection of the radial eigenvalue problem (27). The "first hyperbolic region" in MHD occurs when K is negative and near zero. This hyperbolic region is completely removed in GCP by the near-elimination of the slow wave.

We have seen that the slow waves behave very differently in GCP and fluid theories. However, the Alfvén continuum remains essentially unchanged; $A = \rho\tilde{\omega}^2 - \sigma F^2$ contains no kinetic integral, neither is it affected by parallel viscosity. Thus, the continuum frequencies are real, and at an Alfvén resonance $r = r_A$ (where $A = 0$ and $F \neq 0$), ξ_r and p_* are both proportional to $\log(r-r_A)$, independent of the model used for the parallel dynamics. However, the discrete Alfvén eigenmodes become weakly damped in GCP.

III. Local stability

III.A The Suydam index

In MHD, the stability to modes localized at the resonant surfaces can be examined by means of an indicial equation analysis. Proceeding along this line, we expand (27-28) around the resonant surface, $r = r_0$, where $F = 0$, with $\tilde{\omega}(r_0) = 0$, and set

$$\xi_r = \xi_0 x^\nu \quad , \qquad p_* = p_0 x^{\nu+1} \quad , \qquad x = r - r_0 \quad .$$

The characteristic exponent can be written as

$$\nu = -\frac{1}{2} \pm \left(\frac{1}{4} - D_0\right)^{1/2} = -\frac{1}{2} \pm is \quad .$$

When D_0 is real, as in MHD or CGL, $D_0 > 1/4$ implies the existence of an infinite sequence of unstable eigenmodes,[14] and $D_0 < 1/4$ is a necessary condition for stability, as shown by Suydam.[22] The Suydam index for the generalized system (27-28) is given by

$$D_0 = \frac{1}{\sigma - M^2} \left(\frac{q}{q' B_z}\right)^2 \{ - 2MV \frac{B_z^2}{r B_\theta} \frac{q'}{q}$$

$$- \frac{B^2}{B_\theta^2} [r (\frac{V^2}{r^2})' + \frac{a_4}{\rho r^2} (V - MB_\theta)^4] \qquad (29)$$

$$+ \frac{1}{r^2} [- r (p_{||}' + p_\perp') + H^2 / K B_\theta^2 - (\sigma + M^2) B_\theta^2 + 2(V - MB_\theta)^2] \},$$

where prime denotes differentiation with respect to r. In Eq. (29),

$$M = \sqrt{\rho}\, \tilde{\omega}' / F' = \frac{\sqrt{\rho}\, d/dr(\underline{k} \cdot \underline{v})}{d/dr(\underline{k} \cdot \underline{B})} \quad , \qquad (30)$$

is the differential Mach number. Furthermore, we have introduced

$$V = \sqrt{\rho}\, v_\theta \quad . \qquad (31)$$

and the usual safety factor $q = rB_z/RB_\theta$, where R is an assumed major radius. The phase velocity

$$V_p = - M v_A \quad , \qquad (32)$$

entering the arguments of the Z-function, is real. The MHD expression[7] for D_0 is recovered after some algebra by substituting Eq. (B2) for a_1 through a_4. In Appendix C we compare the Suydam criteria of the three models in the case of non-sheared flow M=0. As is well known,[23] the CGL condition is more optimistic than MHD, but MHD with $\gamma = 1$ reproduces the isotropic GCP condition exactly in the absence of sheared flow. We also show that the Suydam criterion for MHD with infinite parallel viscosity is more optimistic than its CGL counterpart.

When the flow is has shear, the guiding centre result differs from its fluid counterparts in two essential ways. First, in MHD, D_0 has a singularity due to resonance with the slow magnetoacoustic waves[7]

$$D_{res}^{MHD} = \left(\frac{q}{q'B_z}\right)^2 \frac{[(V-MB_\theta)^2 + M^2(B_\theta^2 - V^2)]^2}{(1-M^2)\, r^2 B_\theta^2} \frac{1+\beta}{\beta - M^2(1+\beta)} \,.$$

In GCP the resonance is broadened kinetically. The slow wave continuum still appears through the terms $\propto K^{-1}$ in C_1 to C_3, but the zeroes of K now correspond to oscillations that are damped in time. Since $K^{-1} = 1 + O(\beta)$ for all real phase velocities in GCP, we can assert that the term in D_0^{GCP} representing the interaction with the slow magneto-acoustic wave is small in a low-β plasma with sub-Alfvénic flows. The same conclusion could have been drawn with less effort if we had crudely added an imaginary part of order β to the resonant denominator, $\beta - M^2(1+\beta)$, in D_{res}^{MHD}.

The other modification, perhaps more of theoretical interest, is that the Suydam parameter in GCP becomes complex whenever M is nonzero. As a consequence, the infinite sequences of unstable eigenmodes occurring in MHD when $D_0 > 1/4$ no longer exist. An asymptotic analysis similar to that in Ref. 7 now predicts that the growth-rates lie on spirals in the complex plane, $\Gamma_n = i\tilde{\omega}_n(r_0) = \Gamma_0 \exp(-n\pi/s)$, n = 1,2,.., with $s = (D_0 - 1/4)^{1/2}$ complex. The spiral will eventually cross the real ω-axis and the higher modes will be damped. (When the sequence reappears on the unstable side, it is on an unphysical Riemann sheet, corresponding to an integration path in the complex r-plane that cannot be deformed to the real axis, and so must be discarded.) Thus, when D_0 is complex, no truly asymptotic statement can be made concerning the existence of unstable modes. Evidently, the complex Suydam parameter of GCP does not have as clear an interpretation as its realvalued MHD counterpart.

III. B Discrete slow modes

The MHD Suydam criterion predicts unconditional instability when M^2 approaches $\beta/(1+\beta)$ from below. As we have shown, this loss of stability does not occur in GCP. MHD theory[7] also predicts that as M^2 is increased just above $\beta/(1+\beta)$, the subsonic instabilities transform into infinite sequences of unstable discrete slow

modes, accumulating at the edge of the slow wave continuum, where K has a quadratic zero in r.

In the guiding centre description, the slow wave continuum, K = 0, lies in the stable halfplane (except at $k_{||} = 0$, where it touches the real axis) and infinite sequences of unstable slow modes cannot exist, for several reasons. First, as in the Suydam case, the D parameter, determining the characteristic exponent, is complex in GCP, and consequently the sequences can only be finite. Secondly, if an infinite sequence does exist, its accumulation frequency will lie in the stable halfplane. We may expect that in most cases, even the low order discrete slow modes that are potentially unstable in MHD,[7] are stable in GCP, if they exist at all. (Of course, if a locally unstable particle distribution is chosen, K can have zeroes in the unstable halfplane, giving rise to an unstable slow wave continuum.) Thirdly, as K^{GCP} is complex, the equilibrium profiles for which it has a quadratic zero for any ω, is a set of measure zero. Stated differently, the complex slow wave continua in GCP do not have "edges".

We conclude that the guiding centre spectrum is genuinely different from that of MHD with respect to anything related to the slow waves, and for non-zero M, these differences have important consequences for stability.

III. C Numerical results

To see numerically the effects of flows on the local modes, we have computed the growth-rate of the most unstable mode for an RFP equilibrium varying the pressure and axial flow. The equilibrium has minor radius a = 1 and

$$
\begin{aligned}
&B_\theta = J_1(\lambda r) \quad , \qquad B_z = J_0(\lambda r)\,[1 - 2P_0\sigma(r_0 - r)]^{1/2} \quad , \\
&\rho = 1 - 0.9r^2 \quad , \qquad p = P_0\, J_0^2(\lambda r)\,\sigma(r_0 - r) \quad , \\
&v_\theta = 0 \quad , \qquad v_z = v_{z0}\,(1 - r^2) \quad , \\
&\lambda r_0 = 2.40483 \quad (= \text{first zero of } J_0) \quad , \qquad \lambda = 2.8 \quad ,
\end{aligned}
\tag{34}
$$

where σ now denotes the Heaviside step-function. The mode has m = 1 and k = 2.4. The result is shown as plots of constant growth-rate in Figs. 2a (GCP) and 2b (MHD).

As noted in Ref. 7, MHD gives very pessimistic predictions for marginal stability when the flow is about sonic. However, Fig. 2b shows that the growth-rate of the flow driven instability can be extremely small and clearly outside the region where ideal MHD is reliable. By contrast, GCP predicts that the flow somewhat increases the pressure gradient stable to local modes. It also makes the marginal stability boundary more sharply defined at finite flow speed as is seen from the piling up of the contours of with increasing v_z in Fig. 2a. The main difference between the stability diagrams 2a and 2b is that the region around the sound speed, that is weakly unstable even for small pressure gradients in MHD, becomes stable in the guiding centre description. However, also at a more robust growth-rate, 10^{-2}, GCP and MHD give opposite results with respect to the influence of flow on the allowable pressure gradient. In GCP, sheared flow can be favorable for local stability, due, in part, to the kinetic damping.

III. D Large aspect ratio limit

For toroidal devices, the Suydam criterion must be replaced by the Mercier criterion, which still remains to be worked out in the presence of mass flow. However, certain information relevant to tokamaks can be obtained from the Suydam criterion (29) by considering a large aspect ratio ordering, $\beta = O(\varepsilon^2)$, $B_\theta/B_z = O(\varepsilon)$. It is seen directly from the GCP expression for D_0 that sonic flows [i.e., we assume that M, $V/B_\theta = O(\varepsilon)$] only give $O(\varepsilon^2)$ contributions to D_0, which must be discarded because of the ordering. Notably, the same conclusion cannot be drawn in the inviscid fluid models, because of the unphysical resonance with the slow magneto-acoustic wave. However, for Alfvénic flows [M, $V/B_\theta = O(1)$], D_0 will be order unity also in GCP and consequently relevant information can be extracted. [It must be remembered, however, that the assumed ordering implies $\rho v_z^2/B_z^2 = O(1)$, and that in a toroidal system, such flows can cause ballooning instability because of the toroidal curvature. Moreover, it is necessary to

assume $\beta = O(\varepsilon)$ to avoid equilibria with pathological density distribution within the magnetic surfaces.] In the lowest order, only the three first terms in (29) contribute

$$D_0^{(0)} = \frac{1}{1-M^2} \left(\frac{q}{rq'B_\theta}\right)^2 \left[- 2MVB_\theta \frac{rq'}{q}\right.$$

$$\left. - r^3 \left(\frac{V^2}{r^2}\right)' - \frac{a_4}{\rho} (V - MB_\theta)^4 \right] \quad . \tag{35a}$$

The second term in square brackets is essentially that which determines the stability of an unmagnetized fluid between two rotating cylinders, where the angular frequency v_θ/r must increase outward for ideal stability.[24] From the properties of the Z-function [or by using the fluid equivalent (B2)], we see that $a_4 \approx - \rho/p$ for $M^2 << \beta$ and $a_4 \sim \rho/B^2M^2$ when $M^2 >> \beta$. Thus, the term involving a_4 can be discarded, except when $M^2 < \beta$ and the crossfield flow $V - MB_\theta$ is $O(\varepsilon)$. In this case, the real part of a_4 is negative, hence the a_4 term is destabilizing. (In the opposite case, $M^2 >> \beta$, the term is stabilizing but "small".) If β is ordered as ε, the a_4 term can always be neglected to lowest order, and (35a) can be written in a more transparent form

$$D_0^{(0)} = \frac{-(q/q'B_\theta)^2}{r(1-M^2)} \left(\rho' v_\theta^2 + \frac{2B_\theta}{B_z} \rho v_\theta v_z'\right) \quad . \tag{35b}$$

For definiteness, we assume that B_θ and B_z and v_z are positive and the flow profile is monotonic with v_z vanishing at the edge, so that $v_z' < 0$. According to (35b), this implies that azimuthal flow in the range $-2B_\theta \rho v_z'/\rho' B_z < v_\theta < 0$ is stabilizing. Thus, the flow must be Alfvénic and have the <u>opposite</u> pitch as the magnetic field to give an O(1) stabilizing contribution to D_0. We note that the normal inward density gradient is destabilizing in the presence of azimuthal flow.

IV. Global modes

IV. A Boundary conditions and energy integral

For free boundary modes, the solution of (27) must be matched to a vacuum (or cold plasma) solution with $Q = \nabla\phi$, $p_\perp = p_{||} = 0$. The boundary condition for (27) is continuity of Q_r and $\delta p_\perp + B\delta B$ at the surface, giving

$$p_* = \xi_a \left\{ \frac{1}{a} [(\sigma B_\theta^2 - \rho v_\theta^2)_p - (B_\theta^2 - \rho v_\theta^2)_v] - F_p F_v \frac{\phi}{\partial\phi/\partial r} \right\}_a , \qquad (36)$$

where subscript p and v refer to plasma and vacuum respectively. Equation (36) allows for discontinuities at the surface and also for finite flow of the edge plasma. Integrating $d/dr(p_* r\xi_r)$ from the centre to r = a using (27) and (36), we obtain

$$\xi_a^2 \left\{ [(\sigma B_\theta^2 - \rho v_\theta^2)_p - (B_\theta^2 - \rho v_\theta^2)_v] - F_p F_v \frac{a\phi}{\partial\phi/\partial r} - \frac{(aC_1 - 1)}{C_2} \right\}_a$$

$$= - \int_0^a [\, f \xi'^2 + g \xi^2 \,] \, dr \quad , \qquad (37a)$$

with

$$f = \frac{r}{C_2} \quad , \qquad g = r^2 \left(\frac{rC_1 - 1}{r^2 C_2} \right)' - rC_3 + \frac{rC_1^2}{C_2} - \frac{1}{rC_2} \quad , \qquad (37b)$$

which corresponds to the energy integral δW in the static case. The second order radial equation corresponding to the Hain-Lüst equation[25] in the static case,

$$(f \xi')' - g \xi = 0 \quad ,$$

together with the boundary condition (36) are variational derivatives of (37) with respect to ξ.

As the system with flow is nonselfadjoint, the integral (37) is not as useful as δW for the static problem. However, for a certain class of modes, namely, those locked to resistive walls, Eq. (37) gives valuable information. Such external modes, whose magnetic field has time to diffuse through a resistive wall, have growth-rates of the order of the resistive decay time τ_w (=L/R) of the wall, which is typically much longer than the Alfvén time. Therefore, the frequency of a wall-locked non-resonant mode (i.e., one that does not have a resonant surface in the plasma) can be considered as zero inside the plasma. Thus, Eq. (37) with $\omega = 0$ in f and g may be regarded as an expression for $\phi(\partial\phi/\partial r)^{-1}$ which determines the growth-rate of the resistive wall modes by controlling Δ' at the wall.[26]

IV. B Tokamak ordering

We now apply the analysis of Sec. IV.A in the large aspect ratio, low-β tokamak ordering already discussed for the Suydam criterion, assuming $\beta=O(\varepsilon^2)$, $B_\theta/B_z = O(\varepsilon)$, $\rho v_\theta^2/B_\theta^2 = O(1)$, $\rho v_z^2/B_z^2 = O(1)$. For simplicity, we once again discard the term proportional to a_4, which is correct if the flow is supersonic. (If this term were kept, it would be destabilizing for subsonic flows, as in the case of local modes.) Within the large aspect ratio ordering, the vacuum field is represented as $\underline{Q} = \nabla\psi \times \hat{z}$, and ϕ/ϕ' is translated as $rQ_\theta/imQ_r = (r^2/m^2)\,\psi'/\psi$. For equilibria that are continuous at the surface r=a, the long-thin approximation of (37) with $B_z(r) \approx$ constant becomes

$$\xi_a^2 \left[a^3 F^2 \Delta_\psi + B_\theta^2 (m^2 - n^2q^2) - \rho v_\theta^2 m^2 + \rho a^2(\omega - kv_z)^2 \right]_a$$

$$= \int_0^a (f\,\xi'^2 + g\,\xi^2)\,dr = \delta W_p \quad , \tag{38}$$

where

$$f = r^3(F^2 - \rho\tilde{\omega}^2) \quad ,$$

$$g = r(m^2 - 1)(F^2 - \rho\tilde{\omega}^2) + r^2 \frac{d}{dr}[\rho(\omega - kv_z)^2] \quad , \qquad (39)$$

$$F = (B_\theta/r)(m - nq) \quad , \quad \Delta_\psi = \psi'/\psi|_{r=a} \quad .$$

Equations (38-39) are the standard, "straight tokamak",[27,28] or lowest order reduced-MHD[29] ordering of the linear stability problem for equilibria with Alfvénic flows.

For the wall-locked modes, we must set $\omega = 0$ in f and g. If the wall is modeled as a thin finitely conducting shell, located at r = b, the logarithmic derivative of ψ depends on the frequency according to[30]

$$\Delta_\psi(\omega) = \frac{\Delta_\psi(0) + p\,\Delta_\psi(\infty)}{1 + p} \quad , \quad p = \frac{i\omega\tau_w}{|m|}\left[1 - \left(\frac{a}{b}\right)^{2|m|}\right] \quad ,$$

$$\Delta_\psi(0) = -\frac{|m|}{a} \quad , \quad \Delta_\psi(\infty) = -\frac{|m|}{a}\,\frac{1 + (a/b)^{2|m|}}{1 - (a/b)^{2|m|}} \quad . \qquad (40)$$

Equation (40) shows that the growth rate of a resistive wall mode increases with decreasing Δ_ψ. As a consequence, flow inside the plasma is destabilizing for two reasons, which can be seen from Eqs. (38-39). First, the effect of the field bending F^2 is reduced by the inertial contribution $\rho\tilde{\omega}^2$. (In the present discussion we assume that $\rho\tilde{\omega}^2 < F^2$, otherwise it would be necessary to consider coupling to the continua.[7]) Furthermore, if the axial flow speed decreases toward the edge, the contribution $r^2k^2(\rho v_z^2)'$ to g is also negative, i.e., destabilizing. The only possibility of stabilization by mass flow is if the flow speed is finite at the edge. It is clear from (38) that finite azimuthal flow at the edge is stabilizing. Unfortunately, such profiles appear difficult to

achieve in practice.

IV. C Numerical results

In this section, we give numerical results for global modes obtained from the full system (27) with the boundary condition (36). Figure 3 shows the effect on an m=2, n=1 external kink mode of adding a flow $v_z = v_{z0}(1-r^2)$ to a tokamak-like equilibrium with R/a = 10, q_a = 1.86 and q_0 = 1.05. The wall is located at r=b=1.15a and its time-constant is $\tau_w = 10^4\,\tau_A$. The mode is unstable already in the absence of flow, and Fig. 3 shows that the growth-rate is increased by the flow. The curves are labeled: (a) no azimuthal flow, (b) $v_\theta = v_z kr/m$, giving $\underline{k}\cdot\underline{v} = 0$, and (c) $v_\theta = - v_z kr/m$. Curve (b), for the case of vanishing Doppler shift, shows destabilization by the outward decrease in v_z^2. The destabilization by inertia is also evident, since (c) is the most unstable case. In addition, curve (c) suggests that the instability changes character at a certain flow speed. This is better seen in Fig. 4, where the growth-rates of case (c) in Fig. 3 are shown for three different wall-times: (a) $\tau_w = 10^3\,\tau_A$, (b) $\tau_w = 10^4\,\tau_A$, and (c) $\tau_w = 10^5\,\tau_A$. The transition at $v_{z0} \approx 0.4$ corresponds to the onset of instability with an ideal wall. An interesting feature in Fig. 4 is that for this profile, the growth-rate of the ideal mode shows a minimum when the flow is about Alfvénic.

Figure 5 shows the growth-rate of an internal m=1 kink for a similar equilibrium with $q_0 = 0.95$ and $v_\theta = v_z kr/m$. Figure 6 shows the growth-rate of an m=1 external mode for the RFP equilibrium (34) with $P_0 = 0.03$ and purely axial flow. In this case, k= - 0.6, the wall is located at b=1.1a and its time constant is $10^4\,\tau_A$.

It is evident from Figs. 3-6 that mass flow increases the growth rates of the global modes. This is in agreement with the large aspect ratio theory for resistive wall modes in section IV.B. The numerics also shows that flow is destabilizing for the cylindrical internal kink and external modes in RFP:s. The curves in Figs. 3-6 only show growth-rates of modes that are unstable in the absence of flow, but we also find that flow tends to reduce the region of stability. Thus, the marginal q_0 for the external kink in Fig. 3 is decreased, and that for the internal kink in Fig. 5 is increased by the flow.

V. Equilibrium problem in two and three dimensions

The calculations presented in Sec. II show many similarities with the GCP calculation of toroidal equilibrium by Dobrott and Greene,[16] and in this section we discuss some important consequences of the linear system (27) for the equilibrium problem in two and three dimensions. In particular, we note that the hyperbolic and elliptic regions for the equilibrium problem depend only on the local properties of the linearized equilibrium equation. This equation is a special case of the linear eigenvalue problem for perturbations having zero frequency in the laboratory frame ω (however, their Doppler shifted frequency is non-zero because of the flow). As the information required is local, we can use the cylindrical eigenvalue problem (27), take the limit of m and k large, keeping only the leading terms

$$\frac{d\xi_r}{dr} = \frac{1}{B^2}\left(\frac{E^2}{A} - \frac{1}{K}\right) p_* \quad ,$$

$$\frac{dp_*}{dr} = A\,\xi_r \quad , \tag{41}$$

From (41) we obtain a radial wave number in the WKB sense,

$$k_r^2 = \frac{1}{B^2}\left(\frac{A}{K} - E^2\right) \quad , \tag{42}$$

which is simply the dispersion relation for the slow and fast magneto-acoustic waves. (As usual, the Alfvén wave, A=0, decouples from this dispersion relation. Note that the r-direction is singled out as that which is perpendicular to both $\underline{B}_0$ and $\underline{v}_0$.)

Since, for $\omega = 0$, K depends on m/r and k only through the ratio m/kr, Eq. (42) shows that GCP is non-dispersive in the short wave-length limit, exactly as MHD and CGL. Thus, if the dispersion relation (42) has solutions with k_r, k and m/r nonzero and all real, the real-space form of the linear equation (41) has real characteristics, along

which discontinuities may be propagated, and the equation is of hyperbolic type. In other words, the equilibrium problem is hyperbolic if k_r^2 given by (42) is positive for <u>any</u> real m and k. The equilibrium problem is elliptic if k_r^2 is negative for all real m and k with $k^2 + m^2/r^2 > 0$.

For the moment, we consider explicitly the axisymmetric case and set k = 0 in (42). Then, the MHD equilibrium equation is elliptic when

$$\frac{(1 - M_p^2)(\beta - M_p^2)}{\beta - M_p^2(1 + \beta)} > - \frac{B_z^2}{B_\theta^2} \quad , \tag{43}$$

where $\beta = \gamma p/B^2$ and $M_p = \sqrt{\rho} v_\theta/B_\theta$ is the poloidal Mach number. [Note that Eq. (43) is the well-known ellipticity condition for the MHD Grad-Shafranov equation[15] and that the first hyperbolic region is narrow in tokamaks, for M_p^2 between $\beta/(1+\beta)$ and approximately $\beta/(1+\beta B_z^2/B^2)$.] The present derivation shows that the first hyperbolic region in MHD occurs because, in a narrow range of Doppler frequency due to the flow, perturbations that have zero frequency in the laboratory frame, can propagate radially as slow MHD waves. This occurs when K is small and negative.

If the restriction to axisymmetry is abandoned, we must consider wave vectors $\underline{k}$ in the plane spanned by $\underline{B}$ and $\underline{v}$, making arbitrary angles θ_B and θ_v with respect to $\underline{B}$ and $\underline{v}$ [related of course by $\cos(\theta_B - \theta_v) = \underline{B} \cdot \underline{v}/Bv$]. In terms of the Alfvén Mach number $M_A = \sqrt{\rho} v/B$, or $\mu = M_A^2 \cos^2\theta_v$ (not to be confused with the magnetic moment), the MHD ellipticity condition can be written as

$$\frac{(\cos^2\theta_B - \mu)(\beta \cos^2\theta_B - \mu)}{\beta \cos^2\theta_B - (1+\beta)\mu} > - \sin^2\theta_B \quad , \tag{44}$$

for all θ_B between 0 and $\pi/2$. This condition will be violated when μ is close to $\beta\cos^2\theta_B/(1+\beta)$, which is satisfied for a suitable direction of $\underline{k}$ when the flow is

supersonic, $M_A^2 > \beta/(1+\beta)$. Moreover, by taking θ_B close to $\pi/2$, the ellipticity condition (B4) can be violated for arbitrarily small μ and, hence, for arbitrarily small flow, unless the flow is field-aligned. Thus, in the three-dimensional case, only field aligned flow gives a finite threshold for hyperbolicity in MHD:

$$\frac{(1 - M_A^2)(\beta - M_A^2)}{\beta - (1+\beta)M_A^2} < 0 \quad . \tag{45}$$

In this case, the equilibrium equation is hyperbolic when $\beta/(1+\beta) < M_A^2 < \beta$ or $M_A^2 > 1$.

However, the MHD system without restriction to axisymmetry is hyperbolic for any non-zero flow across the field lines. Thus, calculations of stellarator equilibria with mass flows require GCP theory (or any other theory that eliminates the slow wave).

The guiding centre result for equilibria with mass flow is entirely different in that $K \approx 1$ in a low-β plasma, and slow magneto-acoustic waves do not exist, except in cases with pathological particle distributions. In Fig. 7, we plot $\mathrm{Re}(k_r^2)$ as a function of M_p for MHD and GCP. Although the equilibrium has high β, $p/B^2 = 0.1$, and small aspect ratio, $r/R = 0.3$, the first hyperbolic region is narrow in MHD. More importantly, it is completely removed in GCP. It may be noted that he absence of the first hyperbolic region in the GCP equilibrium problem[16] is connected with the nonvanishing of the real and not the imaginary part of K since, in toroidal equilibria, the distribution functions must be symmetric in the trapped region (cf. Ref. 16, where the real-valued integral C_* corresponds to our a_1). It is easy to see that if we make the low-β approximation $K \equiv 1$, which is uniformly valid with respect to the flow speed in GCP, then $k_r^2 < 0$ for all $M_A^2 < 1$ even in the general three-dimensional case, i.e., the GCP equilibrium equation remains elliptic as long as the flow is sub-Alfvénic.

VI. Conclusion

The guiding centre plasma model, which treats the motion of the particles along the magnetic field kinetically, gives significantly different results than MHD when the equilibrium has sheared mass flow. In particular, GCP removes the complete loss of stability that occurs in MHD for near-sonic flows. In the present paper, we have applied GCP theory to investigate the ideal stability of cylindrical equilibria.

In the "straight tokamak" ordering, sonic flows have little influence on stability, and the flows must be Alfvénic to have a strong effect in GCP. The leading order contribution to the Suydam criterion is given by Eq. (35). Flows, whose axial component decays monotonically toward the edge, can be stabilizing for the local modes only if the flow has the opposite pitch as the magnetic field. We find numerically for high-β RFP equilibria that flow can be stabilizing for the local modes, apparently due to the kinetic damping of the slow waves.

For external modes locked to resistive walls, we have shown analytically in the large aspect ratio tokamak limit that flow is destabilizing if the velocity goes to zero at the edge (38-39). Numerical evidence supports this conclusion also for RFP:s. Despite numerous attempts, we have not been able to find any flow profile, vanishing at the edge, that improves the stability of the external modes. It is noteworthy, however, that stabilization can be obtained if the edge plasma ($r > a$) rotates in the poloidal direction.

It should be mentioned that weak flows can be stabilizing for global resistive modes when the plasma column has finitely conducting walls. As shown in Refs. 26 and 30, resistive walls can stabilize tearing modes if the Doppler shift due to plasma rotation is large compared with both resistive growth-rates and the inverse of the wall-time. Under these circumstances, the mode cannot diffuse through both the resistive layer and the wall and therefore either the resonant surface or the wall must behave "ideally". Thus, resistive modes can be stabilized by rotation if the plasma is surrounded by walls of finite conductivity. However, sheared flows can also destabilize tearing modes by influencing the dynamics inside the resistive layer.[31]

For the problem of toroidal equilibrium, Dobrott and Greene[16] showed that the guiding centre plasma behaves very differently than the MHD fluid, and that the hyperbolic region for poloidal flows comparable to the poloidal sound speed is removed in GCP. We have shown that this "first hyperbolic region" is due to the propagation of slow MHD waves, that are practically eliminated in GCP. For three-dimensional equilibria, the difference between the kinetic and fluid models is even more dramatic; the MHD equilibrium equation becomes hyperbolic for arbitrarily small flows across the magnetic field, whereas the GCP equilibrium problem remains elliptic as long as the flow is sub-Alfvénic.

Our study has shown that a kinetic description of the parallel dynamics is needed to understand equilibrium and stability of plasma with mass flow. An inevitable, but unfortunate, consequence is that the two-dimensional stability problem in toroidal geometry becomes considerably more difficult than in the static case, as the kinetic equation is non-local along the field lines. (This is, fortunately, easy to deal with in the cylindrical analysis). It appears that an understanding of the stability for rotating plasmas, comparable to the detailed picture that has emerged for static equilibria, will present significant difficulties and remains a major challenge to plasma theory. The cylindrical results indicate that although it is possible to improve on local stability by adding mass flow, depending on details of the profiles, flow is always destabilizing for external kink modes.

Acknowledgement

This work was funded in part by the Fonds National Suisse pour la Recherche Scientifique. We are grateful to Prof. F. Troyon for his continued support and interest in this problem and to Drs. K. Appert and J. Vaclavik for many stimulating discussions.

Appendix A. Energy relations

It is worthwhile to discuss energy conservation in systems with anisotropic pressure, which we show is related to the symmetry $a_2 = a_3$ in Eq. (22). The linear equation of motion (1) has the form

$$\rho \frac{\partial^2 \underline{\xi}}{\partial t^2} + 2\rho\, \underline{v}\cdot\nabla \frac{\partial \underline{\xi}}{\partial t} = \underline{F}[\underline{\xi}] + \underline{G}[\delta p_\perp, \delta p_\parallel] \quad . \tag{A1}$$

The energy balance equation is obtained by dotting (A1) with $\underline{\xi}(\underline{r},t)$ [or, if $\exp(i\omega t)$ dependence is assumed, by taking the real part of the scalar product with $-i\omega^*\underline{\xi}^*$] and integrating. The convection term on the left-hand side of (A1) is an antisymmetric operator acting on $\partial\underline{\xi}/\partial t$, and does not affect the energy balance. For fluid models, where $\delta p_\perp$ and $\delta p_\parallel$ are expressed in terms of $\underline{\xi}$ by an equation of state, energy conservation is equivalent to the condition that $\underline{F}+\underline{G}$ is selfadjoint in terms of $\underline{\xi}$. (Thus, if $\underline{v} = 0$, the eigenvalue problem for such a model is selfadjoint if the system is energy-conserving, but selfadjointness is clearly lost when mass flow is added, whether $\underline{F}+\underline{G}$ is energy-conserving or not.) A necessary condition for conservation of energy within the linear system (A1) is that $\underline{F}+\underline{G}$ be Hermitean for real ω.

In the GCP formalism, $\xi_\parallel$ cannot be treated as a virtual displacement on the same footing as ξ_r and $\xi_\perp$. Rather, $\xi_\parallel$ has to be determined, together with $\delta\rho$, $\delta p_\perp$ and $\delta p_\parallel$, from ξ_r and $\xi_\perp$ (or more conveniently, ξ_r and δB) at an assumed value of ω. We consider the system to be energy conserving if $\underline{F}+\underline{G}$ in (1) is Hermitean when the frequency is real. Dotting (5) with $\underline{\xi}^*$ to produce a quadratic form, we find that one piece is not automatically Hermitean, namely

$$\frac{\delta B^*}{B}\,\delta p_\perp + \left(\frac{\delta\rho^*}{\rho} - \frac{\delta B^*}{B}\right)\left(\delta p_\parallel - \Delta B \delta B\right) \quad , \tag{A2}$$

which gives the parallel and perpendicular contributions to the product of plasma compression and pressure perturbation. By substituting $\delta p_\parallel$ from (15), and $\delta\rho$ and $\delta p_\perp$

from (21), we find that $\underline{F}+\underline{G}$ is Hermitean if $a_2 = a_3^*$ and a_1 and a_4 are real for real ω. The symmetry $a_2 = a_3$ in (22) therefore means that the linear GCP system has an energy integral when the a-coefficients are real, i.e., when the kinetic damping vanishes. Wave-particle resonance introduces damping in the macroscopic system, which corresponds to irreversible conversion of kinetic energy into heat. In the inviscid fluid models, where all the coefficients a_1 through a_4 are real, energy conservation becomes equivalent to $a_2 = a_3$. In Appendix B, we show that this can be formulated as a condition on the partial derivatives of the pressures with respect to ρ and B. The condition is, of course, satisfied by the MHD and CGL equations.

Appendix B. Parallel dynamics in MHD and CGL

In this Appendix, we first derive the coefficients a_1 to a_4 describing the parallel dynamics for fluid models with an equation of state $p_\perp = p_\perp(\rho,B)$, $p_{||} = p_{||}(\rho,B)$ and give the condition for energy conservation, that corresponds to the relation $a_2 = a_3$ for GCP. By differentiating the equation of state, $\delta p_{||}$ may be expressed in terms of $\delta\rho$ and δB and parallel equation of motion (15) then gives $\delta\rho$ in terms of δB and $\xi_r\, \rho X^2/r$, and thus a_3 and a_4. Then, a_1 and a_2 are obtained by differentiating $p_\perp = p_\perp(\rho,B)$. In the inviscid fluid models, all coefficients are real and the condition for energy conservation becomes $a_2 = a_3$, which can be written as a condition on the partial derivatives of the pressures (see also the companion paper[19] on toroidal equilibrium):

$$B\,\frac{\partial(p_{||}/\rho)}{\partial B} = \rho\,\frac{\partial[(p_{||} - p_\perp)/\rho]}{\partial\rho} \quad . \tag{B1}$$

We note that both the MHD and double adiabatic equations satisfy this condition. Other models may be introduced which have the same property, for instance the isothermal model discussed in Ref. 19. When condition (B1) is satisfied, the coefficients corresponding to (22) are given by

$$a_1 + \frac{2p_\perp}{B^2} = \frac{\partial p_\perp}{B\partial B} + \frac{\partial p_\perp}{\partial\rho}\,\frac{\rho}{B^2}\,(1 + a_2) \quad ,$$

$$a_2 = \frac{\partial p_\perp}{\partial\rho}\,a_4 \quad , \qquad a_4 = \frac{1}{V_p^2 - \partial p_{||}/\partial\rho} \quad , \tag{B2}$$

where $V_p = -\tilde{\omega}/k_{||}$ is the parallel phase velocity in the plasma frame.

It is also possible to derive the coefficients a_1-a_4 for MHD with parallel viscosity as used in a recent calculation by Gimblett.[13] This model is valid in the opposite limit as the collisionless guiding centre model, namely, when the Doppler frequency is small

compared with the ion-ion collision time. The pressure is nearly isotropic, but a small anisotropy results from anisotropic compression,[32]

$$\delta p_{\perp} = \delta p + \mu_{||} s \quad , \quad \delta p_{''} = \delta p_{||} - 2\mu_{||} s \quad . \tag{B3}$$

Here $\mu_{||} = 0.96 p \tau_{ii}$ is the parallel viscosity, and

$$s = \hat{b}\cdot\nabla(\underline{v}\cdot\hat{b}) - \underline{v}\cdot(\hat{b}\cdot\nabla\hat{b}) - \frac{1}{3}\nabla\cdot\underline{v} = i\tilde{\omega}\left(\frac{\delta B}{B} - \frac{2}{3}\frac{\delta\rho}{\rho}\right) \quad , \tag{B4}$$

using (3) and (9). It can be shown, using the expressions obtained by Braginskii,[32] that for a cylindrical equilibrium, the parallel viscosity does not contribute to the linear perturbation in the isotropic pressure p. Thus, we substitute (B3-4) with $\delta p = (\gamma p/\rho)\,\delta\rho$ into the parallel equation of motion (15) and obtain the coefficients a_1-a_4:

$$a_1 + \frac{2p}{B^2} = (B^2 S)^{-1}\left[\gamma p V_p^2 + i\tilde{\omega}\mu_{||}\left(\frac{1}{3}V_p^2 - 3\,v_s^2\right)\right]$$

$$a_2 = S^{-1}\left(v_s^2 - \frac{2}{3}\,i\tilde{\omega}\mu_{||}/\rho\right) \quad , \quad a_4 = S^{-1} \quad , \tag{B5}$$

$$S = V_p^2 - v_s^2 - \frac{4}{3}\,i\tilde{\omega}\mu_{||}/\rho \quad , \quad v_s^2 = \gamma p/\rho \quad .$$

Once again, $a_3 = a_2$, although both are complex, and the parallel viscosity has broadened the resonance at the sound speed similar to the kinetic effect in GCP. Since the collisionless models apply for frequencies larger than ν_{ii}, it is of interest to extend the MHD model with parallel viscosity past its region of validity, noting that the coefficients in (B5) have a well defined limit when $\tilde{\omega}\tau_{ii} \to \infty$,

$$a_1 + \frac{2p}{B^2} = \frac{\rho}{B^2}\left(\frac{9}{4}v_s^2 - \frac{1}{4}V_p^2\right) \quad ,$$

$$a_2 = \frac{1}{2} \qquad , \qquad a_4 = 0 \; . \tag{B6}$$

Now, the sound-wave has been completely removed, but the imaginary parts are still lacking, and the dependence on the parallel phase velocity is quite different from that in GCP. Effectively, the plasma has been made more rigid, and only displacements with isotropic compression, giving $\delta\rho/\rho = (3/2)\delta B/B$, are allowed. What used to be the slow wave continuum, $K = 1 + a_1 + 2p/B^2 = 0$, has moved to larger phase velocity, $V_p^2 = 4v_A^2 + 9v_s^2$. This is similar to the incompressible case $\gamma = \infty$, where the "slow wave continuum" becomes degenerate with the Alfvén continuum at $V_p^2 = v_A^2$.

Appendix C. Suydam criteria in GCP, CGL and MHD for shearless flows

For shearless flows (M=0) the kinetic integrals in the Suydam criterion $D_0 < 1/4$ are all evaluated at zero phase velocity, and the coefficients a_1 through a_4 can be taken from Table 1. The Suydam index (29) is split in a natural way as $D_0 = D_{fluid} + D_{kin}$, where D_{fluid} is independent of the kinetic integrals and has the same value in all the models, while

$$D_{kin} = \left(\frac{q}{rq'B_z}\right)^2 \frac{1}{\sigma B_\theta^2} \left(\frac{H^2}{K} - B^2 a_4 \rho v_\theta^4\right) \qquad (C1)$$

is model dependent. As already noted, MHD with $\gamma = 1$ gives the same Suydam criterion as GCP for a distribution in local thermodynamic equilibrium. This was shown in the static case M=V=0 by Pao.[14] To compare the GCP and CGL conditions for anisotropic pressures, we note the inequalities

$$H^{CGL} = \sigma B_\theta^2 - \rho v_\theta^2 (1 - p_\perp/3p_{||}) < H^{GCP} = \sigma B_\theta^2 - \rho v_\theta^2 (1 - p_\perp/p_{||}) \ ,$$

$$K^{CGL} = 1 + \frac{2p_\perp}{B^2} - \frac{p_\perp^2}{3p_{||}B^2} > K^{GCP} = 1 + \frac{2p_\perp}{B^2} - \frac{2p_\perp^2}{p_{||}B^2} \ ,$$

$$-a_4^{CGL} = \rho/3p_{||} < -a_4^{GCP} = \rho/p_{||} \ .$$

Consequently, (assuming $H^{GCP} > 0$ and $K^{GCP} > 0$), each term in D_{kin} is smaller for CGL than for GCP, i.e., $D_0^{CGL} < D_0^{GCP}$ term by term, and the CGL equations are overly optimistic for isotropic, as well as anisotropic equilibria. This also holds in the static case, $v_\theta = 0$, in agreement with the more general comparison between MHD and CGL by Bernstein et al.[23] It appears that the double adiabatic approximation makes the plasma too "stiff" in the longitudinal direction by not allowing the temperatures to

equilibrate along the field lines. Isothermal conditions are simply accounted for in MHD by setting $\gamma = 1$.

We note that the MHD system with an infinite parallel viscosity is even more stiff than CGL. In the isotropic case,

$$H^{MHD}(\mu_{||}=\infty) = \sigma B_\theta^2 - \frac{3}{2}\rho v_\theta^2 \quad < \quad H^{CGL} = \sigma B_\theta^2 - \frac{2}{3}\rho v_\theta^2 \quad ,$$

$$K^{MHD}(\mu_{||}=\infty) = 1 + \frac{9}{4}\frac{\gamma p}{B^2} \quad > \quad K^{CGL} = 1 + \frac{5p}{3B^2} \quad ,$$

$$-a_4^{MHD}(\mu_{||}=\infty) = 0 < \quad -a_4^{CGL} = \rho/3p \quad .$$

so that $D_0^{MHD}(\mu_{||}=\infty) < D_0^{CGL} < D_0^{MHD}(\mu_{||}=0) = D_0^{GCP}$ for plasmas in local thermodynamic equilibrium.

Finally, we give explicitly the GCP Suydam index for isotropic equilibria with M=0,

$$D_0^{GCP} = \left(\frac{q}{q'B_z}\right)^2 \left\{ -\frac{2p'}{r} + \frac{2\rho v_\theta^2}{r^2} + \frac{B^2}{B_\theta^2}\left[\frac{\rho^2 v_\theta^4}{r^2 p} - r\frac{d}{dr}\left(\frac{\rho v_\theta^2}{r^2}\right)\right]\right\} , \qquad \text{(C2).}$$

which shows destabilization by azimuthal flow as well as by an outward decrease in $\rho(v_\theta/r)^2$.

References

1. K. Brau, M. Bitter, R.J. Goldston, D.Manos, K. McGuire, and S. Suckewer, Nucl. Fusion 23, 1643 (1983).
2. R.C. Isler, L.E. Murray, E.C. Crume, C.E. Bush, J.L. Dunlap, P.H. Edmonds, S. Kasai, E.A. Lazarus, M. Murakami, G.H. Neilson, V.K. Papé, S.D. Scott, C.E. Thomas, and A.J. Wootton, Nucl. Fusion 23, 1017 (1983).
3. K.H. Burrell, R.J. Groebner, H. St. John, and R.P. Seraydarian, Nucl. Fusion 28, 3 (1988).
4. The Fluid Mechanics of Astrophysics and Geophysics, Vol 1, "Solar Flare Magnetohydrodynamics", E.R. Priest , Ed., (Gordon and Breach, London, 1982).
5. A.F. Vinas and T.R. Madden, J. Geophys. Res. 91, 1519 (1986); B. Rogers and B.U.O. Sonnerup, ibid., 91, 8837 (1986).
6. E. Hameiri, Ph. D. thesis, New York University, 1976.
7. A. Bondeson, R. Iacono, and A. Bhattacharjee, Phys. Fluids 30, 2180 (1987).
8. A. Bhattacharjee, in Theory of Fusion Plasmas, Proc. workshop, Varenna 1987, (Compositori Editrici, Bologna 1988) p 47.
9. B. Lehnert, J. Bergström, and S. Holmberg, Nucl. Fusion 6, 231 (1966).
10. J.A. Tataronis and W. Grossman, Nucl. Fusion 16, 667 (1976).
11. H. Grad, in Electromagnetic and Fluid Dynamics of Gaseous Plasma (Proc. Symposium , Polytech. Inst. of Brooklyn, 1961) p 37.
12. G. Chew, M. Goldberger, and F. Low, Proc. Royal Soc. (London), A236, 112 (1956).
13. C.G. Gimblett, "The generalization of Newcomb's equation to incorporate parallel ion viscosity and an application to thin shell instabilities", to appear in Plasma Physics and Controlled Nuclear Fusion (1988).
14. Y.P. Pao, Nucl. Fusion 14, 25 (1974).
15. H.P. Zehrfeldt and B.J. Greene, Nucl. Fusion, 12, 569 (1972).
16. D. Dobrott and J.M. Greene, Phys. Fluids 13, 2391 (1970).

17. K. Appert, R. Gruber, and J. Vaclavik, Phys. Fluids 17, 1471 (1974).

18. R. Iacono and A. Bondeson, in Theory of Fusion Plasmas, Proc. workshop, Varenna 1987, (Compositori Editrici, Bologna 1988) p 205.

19. R. Iacono, A. Bondeson, F. Troyon, and R. Gruber, "Axisymmetric Toroidal Equilibrium with Flow and Anisotropic Pressure", (1988) to be submitted to Phys. Fluids.

20. E.A. Frieman and M. Rotenberg, Rev. Mod. Phys. 32, 898 (1960).

21. B.D. Fried and S.D. Conte, The Plasma Dispersion Function (Academic Press, New York, N.Y., 1961).

22. B.R. Suydam, in Proceedings of Second International Conference on the Peaceful Uses of Atomic Energy, Geneva (United Nations, Geneva, 1958), p.157.

23. I.B. Bernstein, E.A. Frieman, M.D. Kruskal, and R.M. Kulsrud, Proc. Roy. Soc. (London), A244, 17 (1958).

24. S. Chandrasekhar, Hydrodynamic and Hydromagnetic Stability (Oxford University Press, London, 1961), Chapter VII; Lord Rayleigh, Scientific papers, 6, 447, Cambridge, England, 1920.

25. K. Hain and R. Lüst, Z. Naturforsch. 13a, 936 (1958).

26. C.G. Gimblett, Nucl. Fusion 26, 617 (1986).

27. V. D. Shafranov, Sov. Phys. - Tech. Phys. 15, 175 (1970).

28. J.A. Wesson, Nucl. Fusion 18, 87 (1978);
J.P. Freidberg, Rev. Mod. Phys. 54, 801 (1982).

29. H.R. Strauss, Phys. Fluids 19, 134 (1976).

30. A. Bondeson and M. Persson, "Stabilization by resistive walls and q-limit disruptions in tokamaks", Nucl. Fusion (to appear 1988).

31. A. Bondeson and M. Persson, Phys. Fluids 29, 2997 (1986).

32. S.I. Braginskii, in Reviews if Plasma Physics, Ed. M.A. Leontovich (Consultants Bureau, New York, 1965) Vol 1, p 205.

TABLE 1

	$-a_1$	$-a_2$	$-a_4$
GCP	$2p_\perp^2/p_\parallel B^2$	$p_\perp/p_\parallel$	$\rho/p_\parallel$
MHD	$2p/B^2$	1	$\rho/\gamma p$
CGL	$p_\perp^2/3p_\parallel B^2$	$p_\perp/3p_\parallel$	$\rho/3p_\parallel$
MHD ($\mu_\parallel=\infty$)	$(2-9\gamma/4)p/B^2$	-1/2	0

Table caption

Table 1. Values of the coefficients a_1, a_2 and a_4, characterizing the parallel motion, in the static limit $V_p = 0$, for GCP, CGL and MHD, including the case of infinite parallel viscosity.

Figure captions

Figure 1 Density response to perturbations in magnetic field strength, $1+a_2$, as a function of the parallel phase velocity for different models of the parallel dynamics: GCP, MHD, and CGL. The solid lines give the real parts and the dashed lines the imaginary parts (= 0 for the fluid models).

Figure 2 Contours of equal growth-rate in GCP (2a) and MHD (2b) for the resonant mode m=1, k=2.4 on the equilibrium (34) with λ=2.8. The MHD description gives rise to a large region of weak instability for near-sonic flows. This region is completely stable in GCP.

Figure 3. Growth-rates of the m=2, n=1 external kink mode vs. flow speed for a tokamak-like equilibrium with q_0=1.05 and q_a=1.86 and a resistive wall at b=1.15a with time constant $\tau_w = 10^4\,\tau_A$. The curves are labeled: (a) no azimuthal flow, (b) $v_\theta = krv_z/m$, giving $\underline{k}\cdot\underline{v}=0$, and (c) $v_\theta = - krv_z/m$.

Figure 4. Growth-rates corresponding to case (c) of Fig. 3 for different wall time constants (a) $\tau_w = 10^3\,\tau_A$, (b) $\tau_w = 10^4\,\tau_A$, and (c) $\tau_w = 10^5\,\tau_A$. For $v_{z0} < 0.4\,v_{A0}$ the mode is a resistive wall instability, whereas for $v_{z0} > 0.4\,v_{A0}$, it is unstable with an ideal wall.

Figure 5. Growth-rate of the internal m=1 kink mode for a tokamak-like equilibrium with $q_0 = 0.95$ and $v_\theta = krv_z/m$.

Figure 6. Growth-rate of the m=1 external mode with k= - 0.6 for the RFP equilibrium (34) with $\lambda = 2.8$, $P_0 = 0.03$ and $v_\theta = 0$. The resistive shell is placed at r = b = 1.1a and has the time constant $\tau_w = 10^4\,\tau_A$.

Figure 7. Square of radial wavenumber in the axisymmetric equilibrium problem vs. poloidal Mach number $M_p = \sqrt{\rho}v_\theta/B_\theta$ in GCP and MHD for an equilibrium with $p/B^2 = 0.1$ and r/R = 0.3. The Grad-Shafranov equation is hyperbolic when $k_r^2 > 0$.

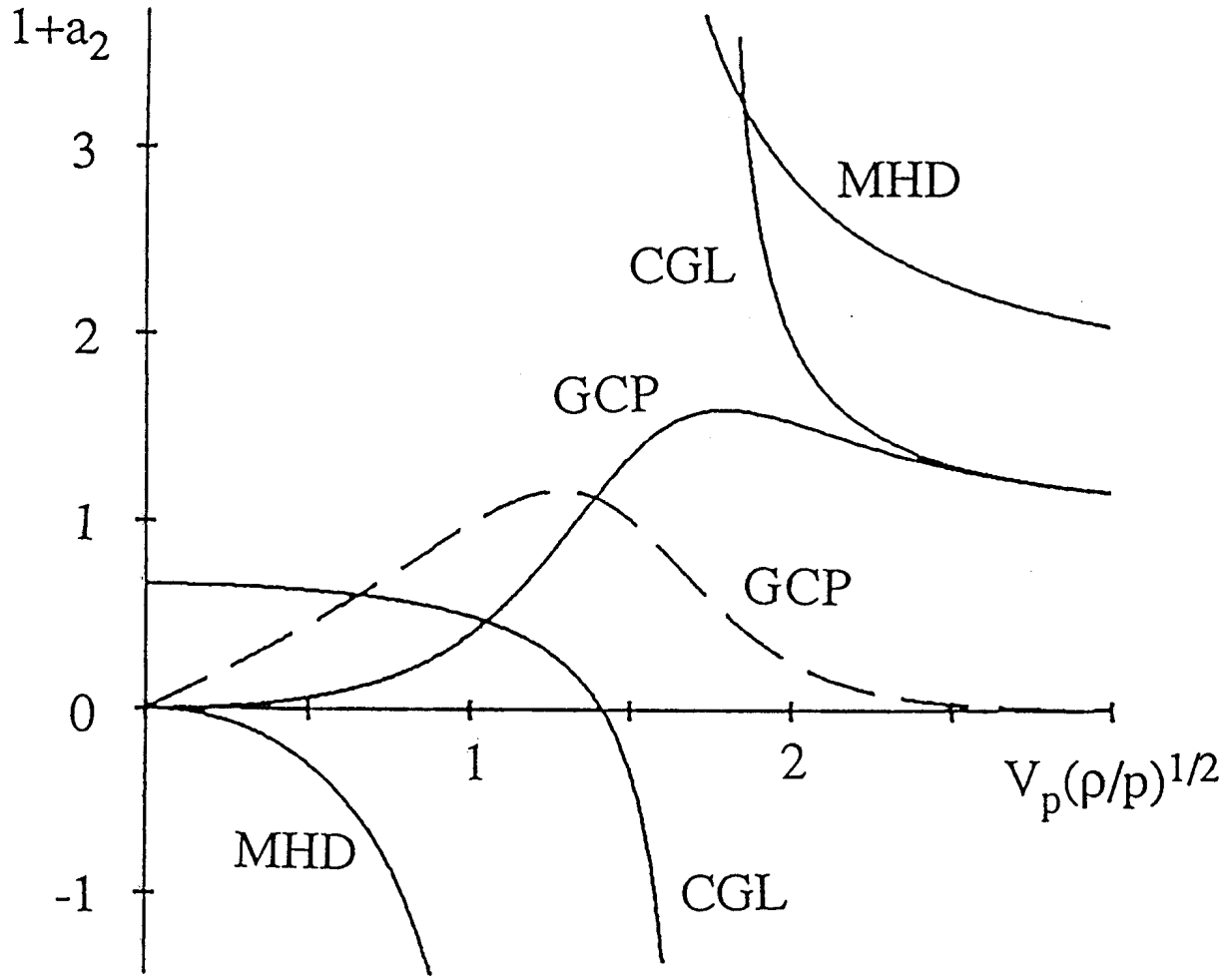

Figure 1

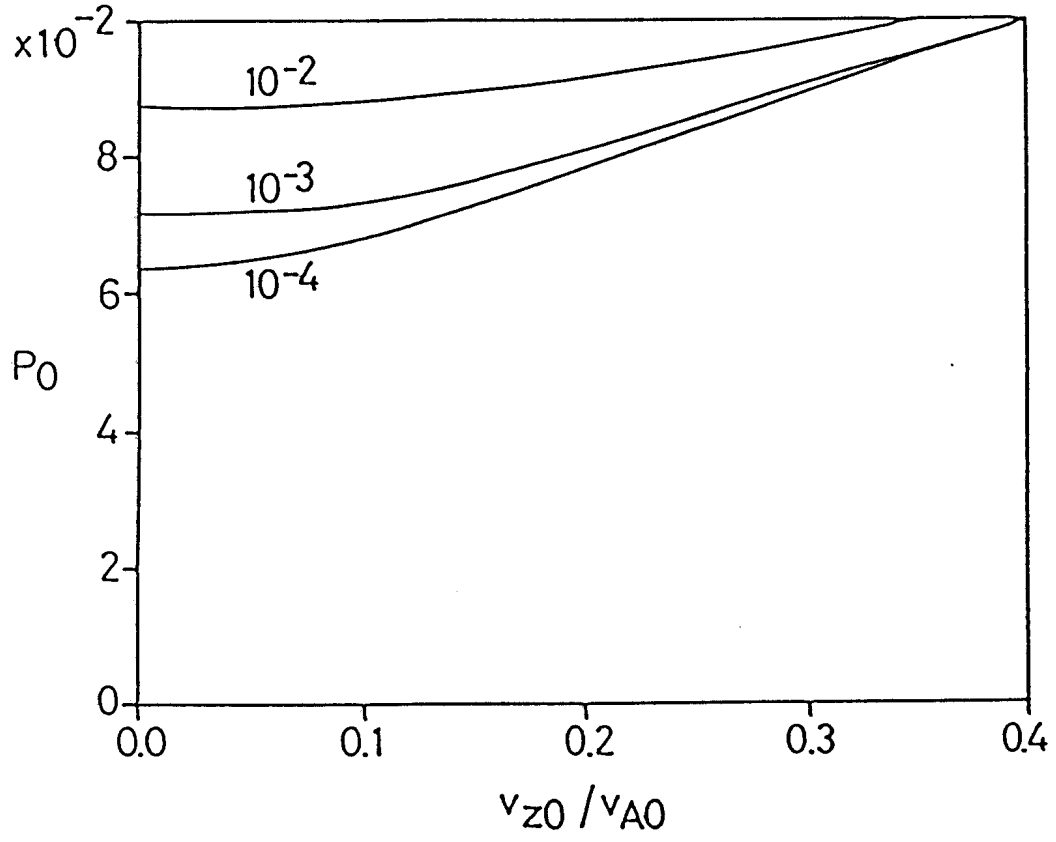

Figure 2a

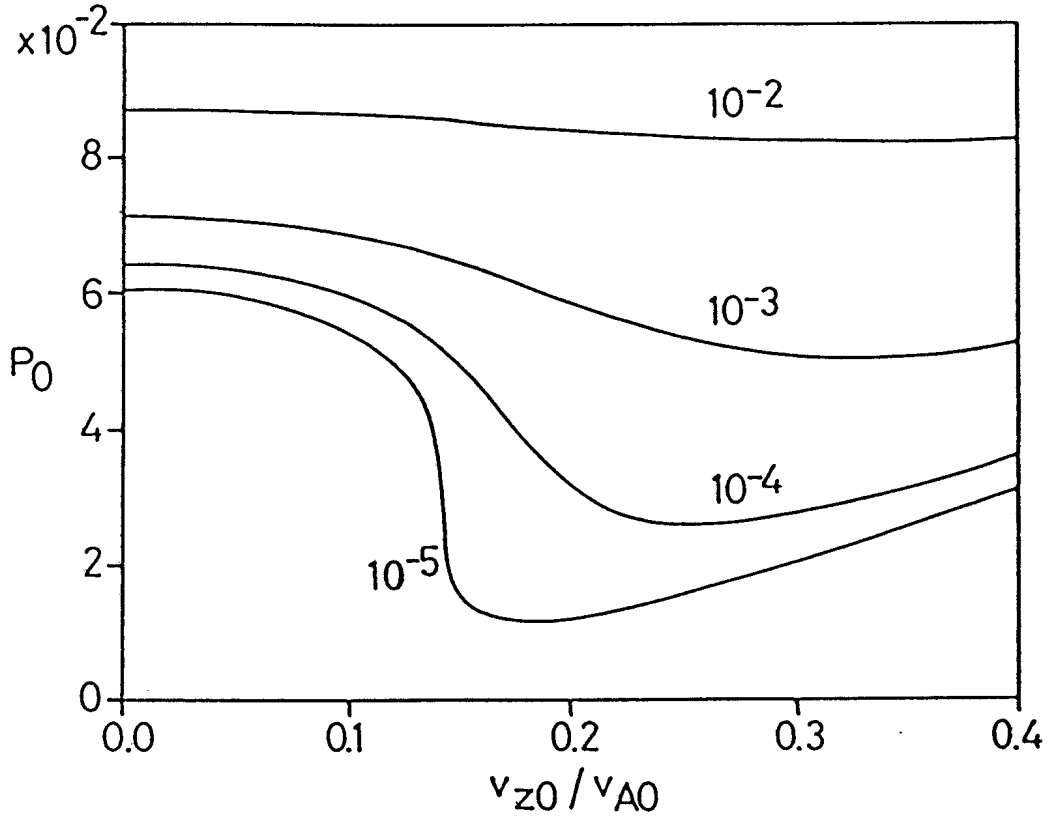

Figure 2b

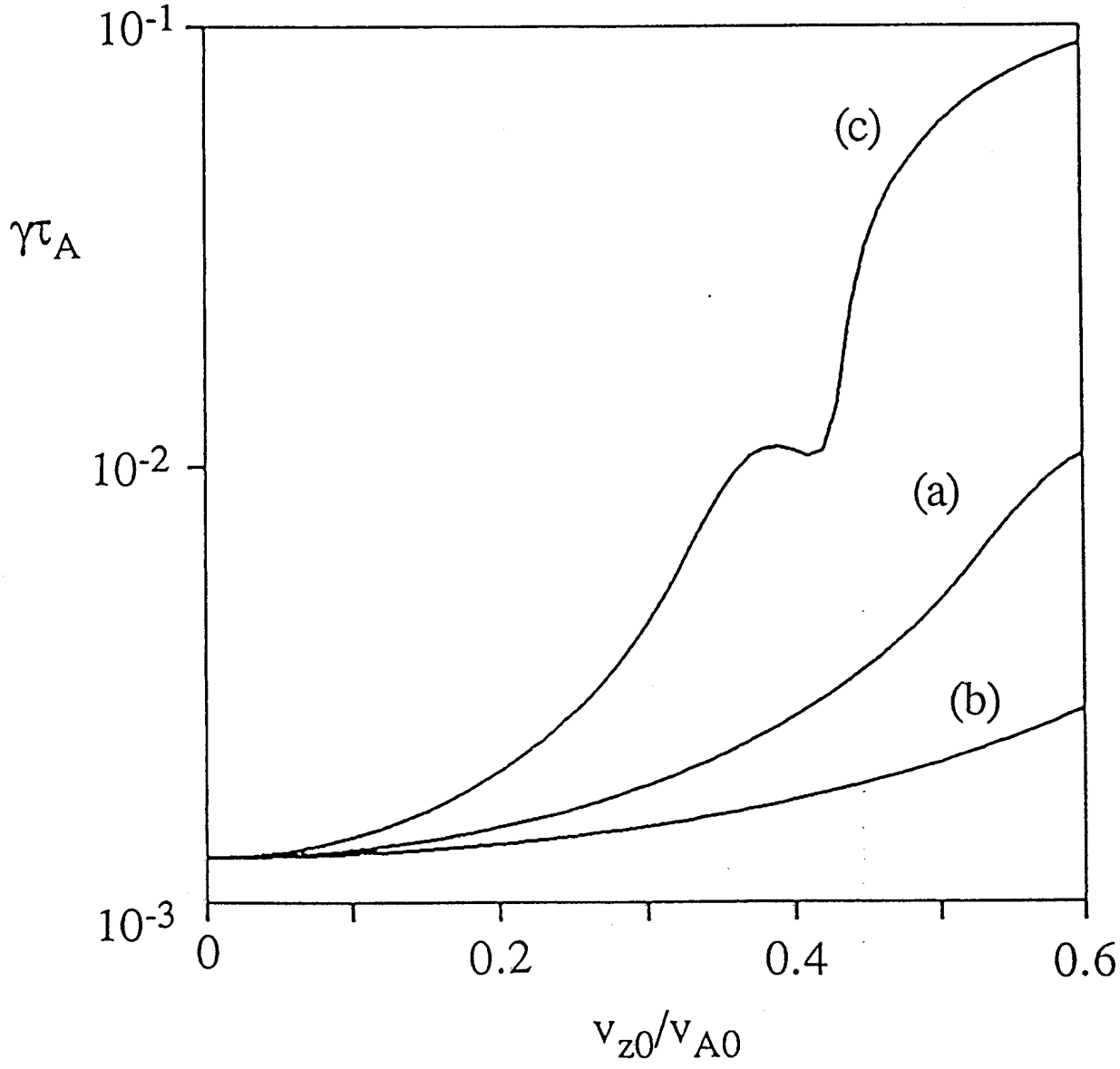

Figure 3

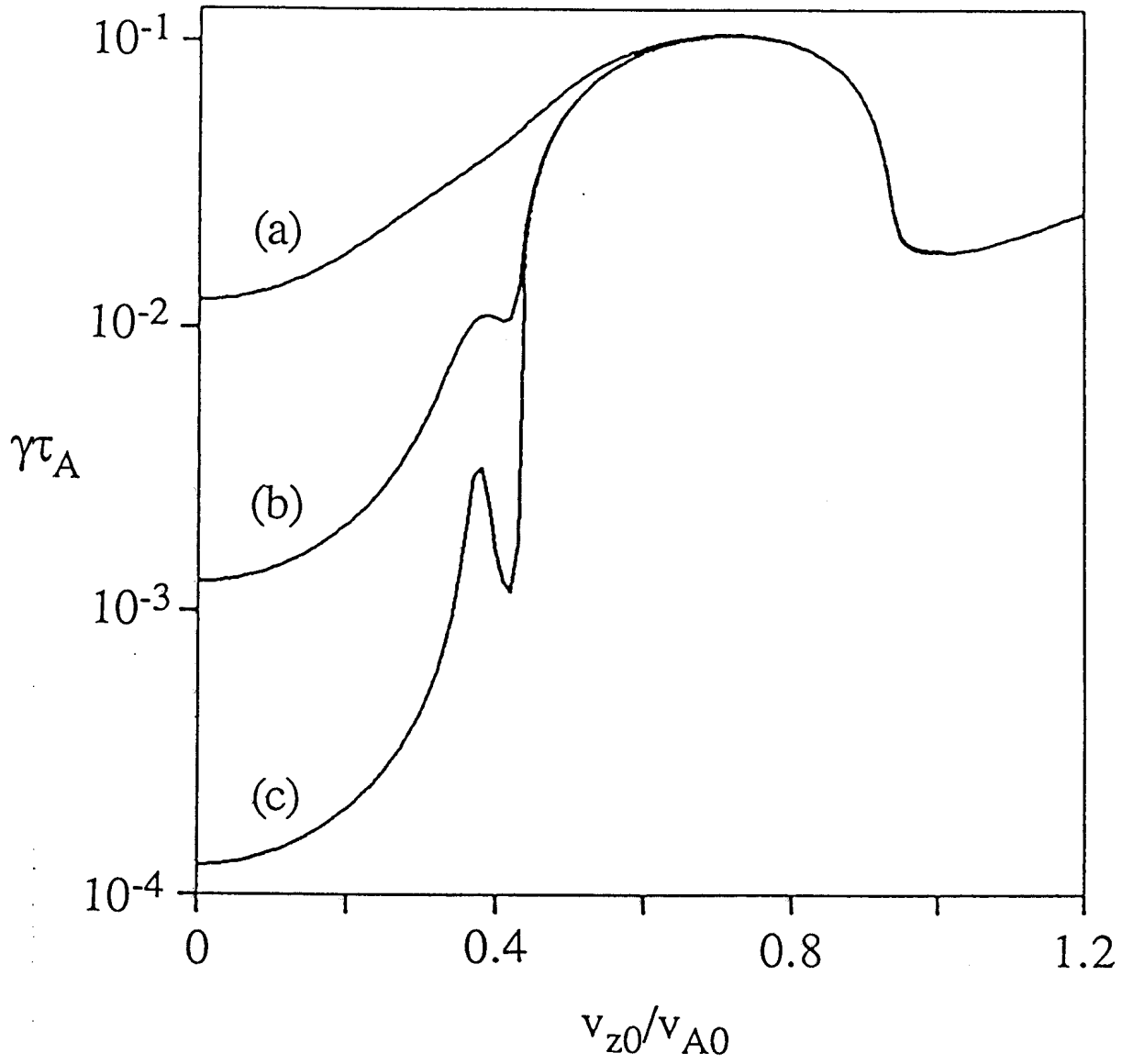

Figure 4

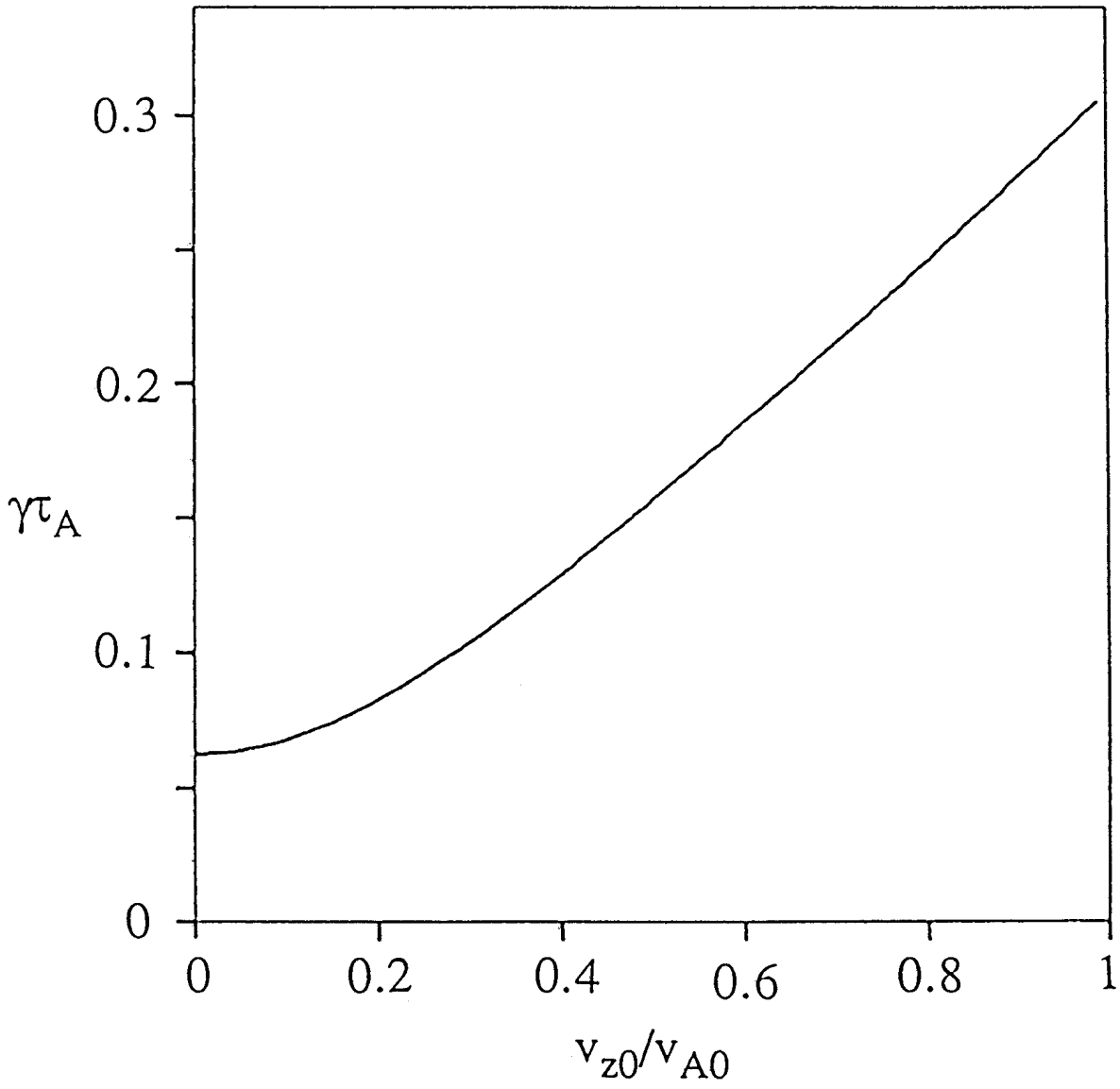

Figure 5

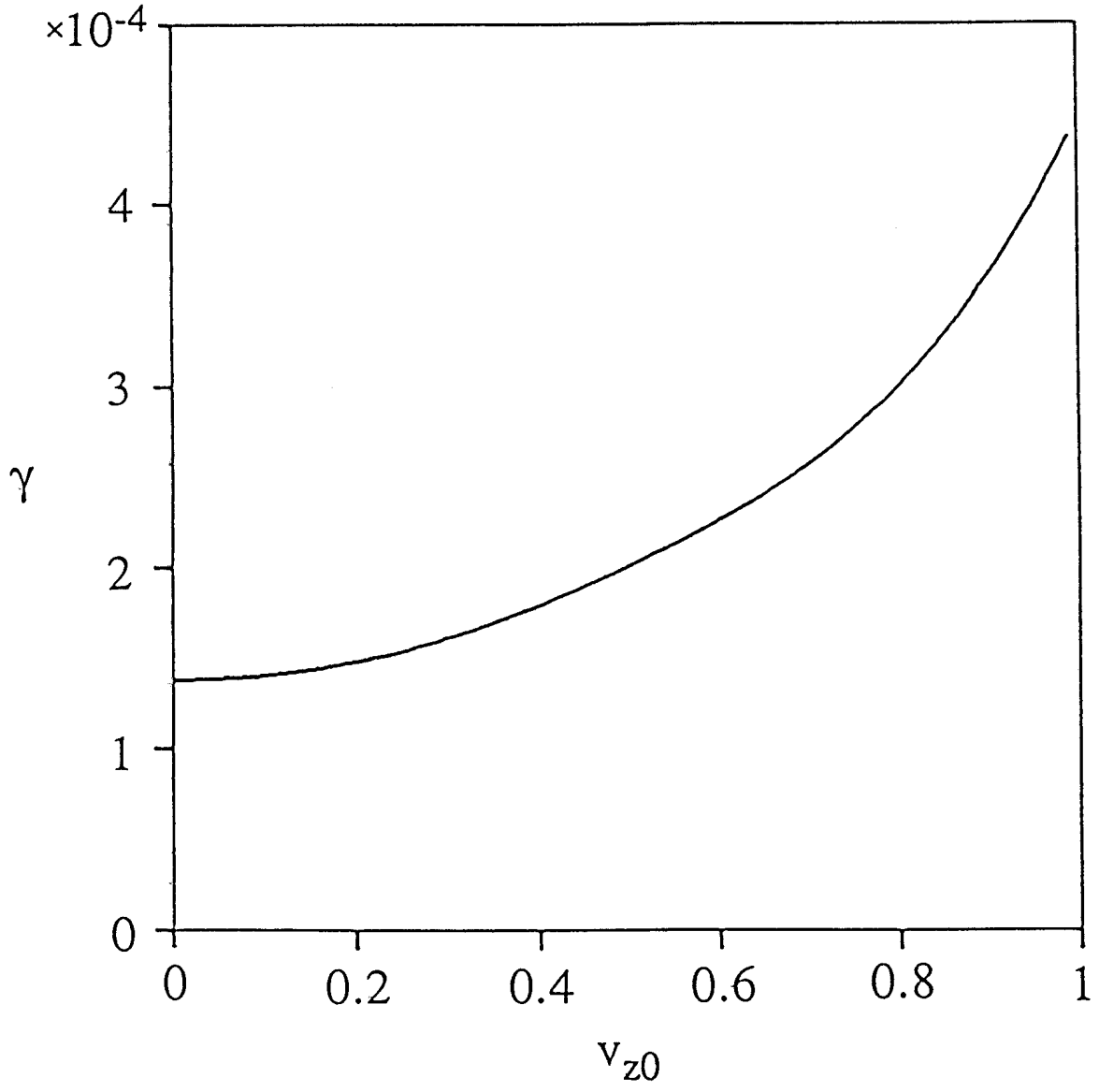

Figure 6

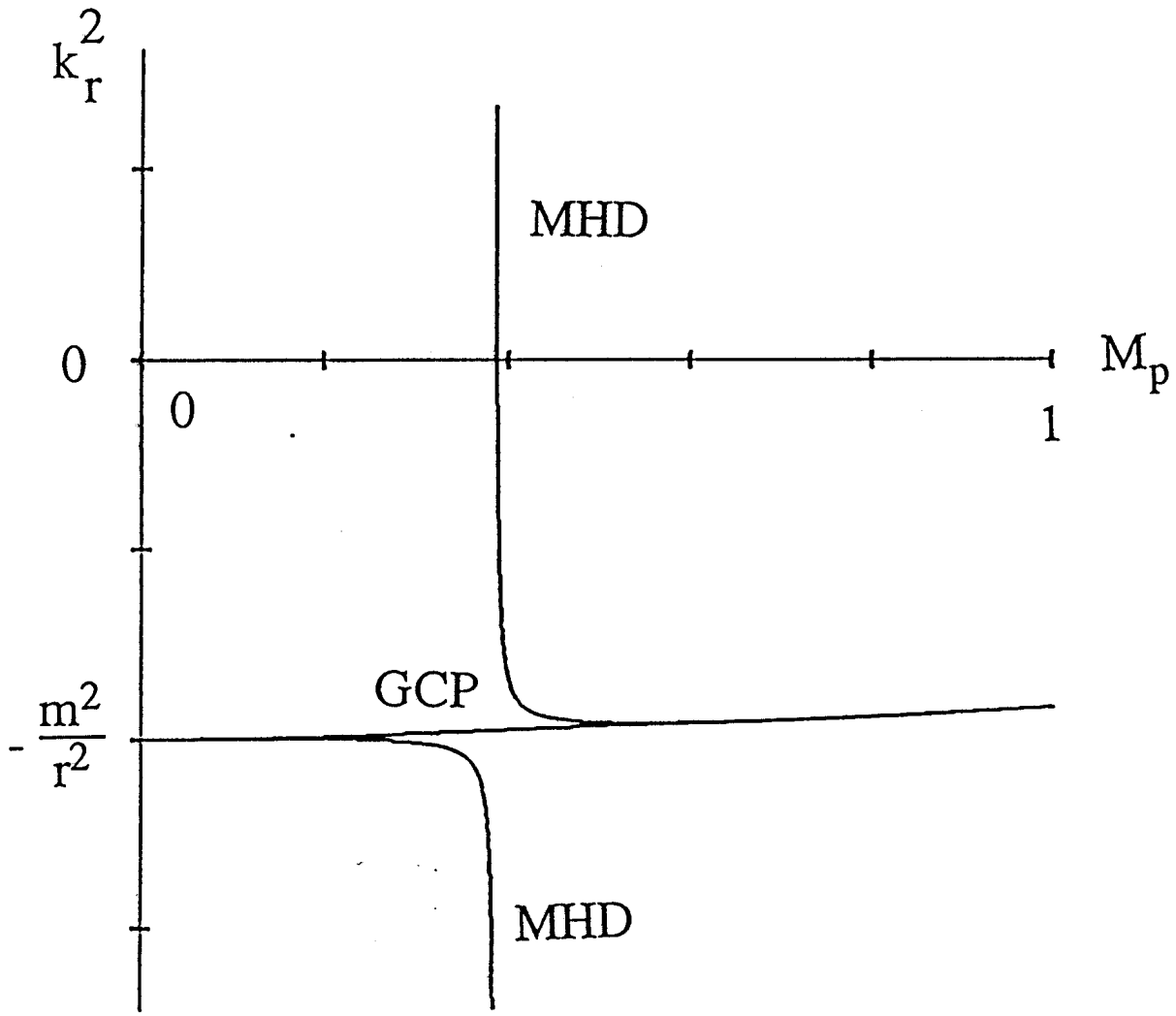

Figure 7